Journal of the Chinese Institute of Engineers, Vol. 23, No. 3, pp. 321-330 (2000)

NUMERICAL SIMULATION OF THE THREE-DIMENSIONAL SLOSHING PROBLEM BY BOUNDARY ELEMENT METHOD

Yung-Hsiang Chen* Wei-Shien Hwang Chia-Hao Ko
Department of Civil Engineering
National Taiwan University
Taipei, Taiwan 202, ROC

Key Words: boundary element methods, liquid sloshing, tuned liquid damper.

ABSTRACT

This study presents a numerical method to describe and predict the phenomena of three-dimensional nonlinear liquid sloshing problem of a tuned liquid damper (or TLD) to any kind of forced motion. The three-dimensional boundary element method with the second-order Taylor series expansion and Lagrangian description is established and used to compute the position and other quantities of the liquid particles in the liquid domain and on the free surface. The calculations of transient solution (or the time history) of the free surface movement and the base shear force from hydrodynamic pressures of a three-dimensional rectangular or cylindrical TLD tank subjected to horizontal harmonic forced oscillation, as two examples, are included in this paper for demonstration and discussion.

I. INTRODUCTION

Sloshing phenomena inside a liquid tank subjected to external motions have been studied for many engineering problems, such as nuclear reactors (Aslam, 1981), huge oil tanks (Velestors, 1984), and tuned liquid dampers (TLD) (Chen *et al.*, 1995; Chen and Hwang, 1994). In most of these cases, the movement of the free surface conducts undesired troubles. But for another case of a tuned liquid damper, the sloshing effect can give a desired reaction force which can reduce the vibration of its main structures. In the present study, our interest is focused on the tuned liquid damper and its reaction force on the main structure.

Two kinds of mathematical models, linear and non-linear models, are frequently used to describe free surface movement. The linear wave model is applied, when the wave amplitude is small. However, as the amplitude of waves becomes larger and larger, the simple linear wave theory is no longer valid. We have to adopt the more complicated non-linear model in order to obtain reasonable results. The present concern is sloshing phenomena and the reaction force for a TLD subjected to any kind of forced motion. In order to achieve better vibration reduction, the waves inside a TLD should be at or close to the resonance condition. At this condition, the elevation of the free surface is no longer small and a non-linear model is necessary.

It is very difficult to solve the non-linear free surface problems analytically, and only a few results have been reported in the research literature. For two-dimensional steady-state conditions, Faltinsen (1974) solved nonlinear sloshing in rectangular tanks. Ikeda and Nakagawa (1997) published their results for the nonlinear vibrations of a structure coupled with sloshing of a rectangular tank. As for the transient

*Correspondence addressee

problem, Chwang and Wang (1984) developed an analytical solution of the hydrodynamic pressure for an accelerating tank, but their approach was limited by a small time expansion. In the meantime, many numerical methods, such as finite element methods, finite difference methods, and boundary element methods (BEM), have been developed. Among those numerical methods, the BEM can efficiently reduce the computational dimensions by one. Such a great advantage of BEM is helpful to reduce computer memory storage, computer computation time, and to make the grid generation easier, especially for three-dimensional computation. Liu *et al.* (1992) applied the BEM and the Taylor Series Expansion to solve two-dimensional sloshing problems. Furthermore, it has been extended to solve wave making problems (Nakayama, 1990), overturning waves (Liu *et al.*, 1992), breaking waves (Grilli and Subramanya, 1996), and the interaction between current and a structure (Bűhmann *et al.*, 1998).

In using the BEM, there are two primary issues of concern. One is the calculation of the velocity or the velocity potential of flow fields. The other is to predict the position of the free surface at every time step. By the assumption of the potential flow, the BEM can directly solve the unknown variables, if enough boundary conditions are given correctly. Two approaches are commonly used to update the free surface condition in the research literature, the Taylor series expansion (TSE) and the Runge-Kutta Method. Machane and Canot (1997) suggested that time stepping based on the Taylor series expansion was more efficient than the Runge-Kutta Method in terms of CPU time. Unfortunately, when the higher-order TSE in time stepping is used, the solution procedure becomes extremely complicated. However, if we don't adopt the higher order TSE method, the TSE method will still be a very practical method for three-dimensional sloshing problems.

Recently, many contributions on the non-linear free surface wave have been obtained by the BEM for two-dimensional cases. Some authors claim their methods can be extended to three-dimensional problems, but unfortunately, only a few examples have been shown. Actually, the handling of three-dimensional problems is not as easy as the two-dimensional ones. The difficulties are mainly due to the complicated geometric simulation, the stability, and increased CPU time (Broeze *et al.*, 1993). However, the three-dimensional analyses are still very important in many engineering problems. In this paper, our interest is concentrated on the numerical calculation of a three-dimensional sloshing problem. The isoparametric quadrilateral linear element is used to model the boundaries of the tank, and the second order TSE with the Eulerian-Lagrangian method is used to track the particles on the free surface. Finally, the transient solution (or the time history) for a three-dimensional nonlinear sloshing problem of a tank to any kind of external forced motion can be calculated. Two examples, the rectangular and cylindrical TLD's to a harmonic forced oscillation, are included for numerical calculation and dicussion.

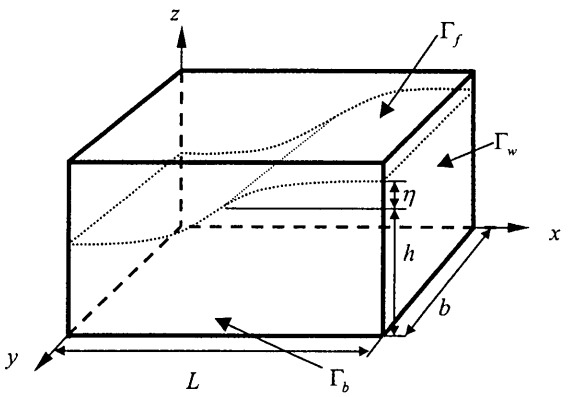

Fig. 1 Model of the calculational region

II. MATHEMATICAL MODELING

The sketch of a liquid tank is shown in Fig. 1. The flow field satisfies the assumptions of potential flow: inviscid, incompressible, and irrotational. The velocity potential is described by the Laplace equation,

$$\nabla^2\phi = \frac{\partial^2\phi}{\partial x^2} + \frac{\partial^2\phi}{\partial y^2} + \frac{\partial^2\phi}{\partial z^2} = 0, \tag{1}$$

in which $\phi(x, y, z, t)$ is the velocity potential in the computational domain Ω. Let u, v, and w be the flow velocities in x, y, and z directions, respectively. Then, by the definition,

$$\frac{\partial\phi}{\partial x} = u\,,\ \frac{\partial\phi}{\partial y} = v\,,\ \frac{\partial\phi}{\partial z} = w\,. \tag{2}$$

In Fig. 1, there are three types of boundaries on the tank: a lateral wall boundary Γ_w, a rigid bottom Γ_b, and a free surface boundary Γ_f. On the free surface, Γ_f, there are two boundary conditions: dynamic and kinematic conditions. Let $\vec{R}$ be the position vector of a particle on the free surface. The kinematic boundary condition on Γ_f is denoted as

$$\frac{D\vec{R}}{Dt} = \left(\frac{\partial}{\partial t} + \vec{U}\cdot\nabla\right)\vec{R} = \vec{U} \quad \text{on } \Gamma_f, \tag{3}$$

in which $\vec{U}$ is the velocity vector of the particle, and

$$\frac{D}{Dt} = \frac{\partial}{\partial t} + \frac{\partial\phi}{\partial x}\frac{\partial}{\partial x} + \frac{\partial\phi}{\partial y}\frac{\partial}{\partial y} + \frac{\partial\phi}{\partial z}\frac{\partial}{\partial z} \tag{4}$$

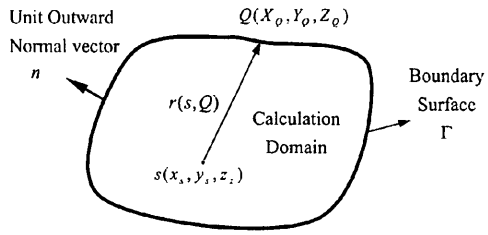

Fig. 2 The calculation domain of boundary integral

represents the time derivative in the Lagrangian description. Hence, the velocity of free surface particles is,

$$\frac{D\overline{R}}{Dt} = \nabla\phi \quad \text{on } \Gamma_f. \tag{5}$$

Let (ξ, ς, η) be the position vector of a particle on the free surface. Then

$$u = \frac{D\xi}{Dt}, \quad v = \frac{D\zeta}{Dt}, \quad w = \frac{D\eta}{Dt} \quad \text{on } \Gamma_f. \tag{6}$$

The other boundary condition of the free surface, the dynamic boundary condition, is the Bernoulli equation:

$$\frac{\partial\phi}{\partial t} + \frac{1}{2}|\nabla\phi|^2 + g\eta + \frac{p_a}{\rho} = 0 \quad \text{on } \Gamma_f, \tag{7}$$

in which g is the gravitational acceleration, η is the altitude of free surface, and ρ is the density of fluid. The atmospheric pressure p_a is taken to be zero. Eq. (7) can be rearranged by the total time derivative as

$$\frac{D\phi}{Dt} = -g\eta + \frac{1}{2}|\nabla\phi|^2 \text{ on } \Gamma_f. \tag{8}$$

In this paper, we only consider horizontal forced vibration, so the normal velocity of the bottom boundary vanishes, i.e.

$$\frac{\partial\phi}{\partial n} = 0 \text{ on } \Gamma_b. \tag{9}$$

Equation (9) is the boundary condition on the bottom boundary Γ_b, and n represents the unit normal vector. In the same way, the lateral wall boundary condition can be assigned as:

$$\frac{\partial\phi}{\partial n} = V_n(x, y, z, t), \text{ on } \Gamma_w, \tag{10}$$

where $V_n(x, y, z, t)$ is the outward normal velocity of the lateral wall boundary.

III. BOUNDARY ELEMENT METHODS

The boundary value problems mentioned in the previous section can be transformed into a boundary integral equation along the tank boundary $\Gamma(\Gamma_f \cup \Gamma_b \cup \Gamma_w)$. As shown in Fig. 2, a field point Q locates at (X_Q, Y_Q, Z_Q) on the boundary, and a source point s locates at (x_s, y_s, z_s) inside the domain. Denoting $G(s, Q)$ as the three-dimensional free-space Green's function of the Laplace Equation, we can write

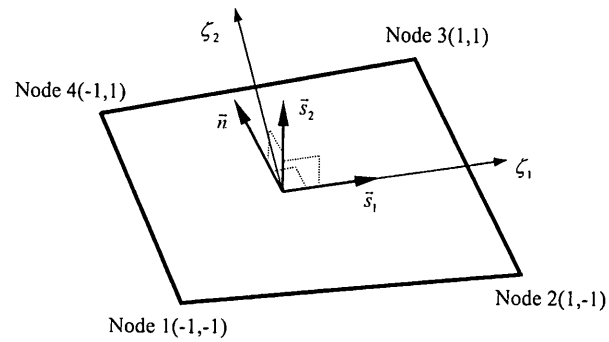

Fig. 3 The quadrilateral linear element and local orthogonal set of axes

$$G(s, Q) = \frac{1}{4\pi}\left[\frac{1}{r(s, Q)}\right], \tag{11}$$

where $r(s, Q)$ is the distance from the source point to the field point. We substitute Eq. (11) into Green's second identity

$$\int_v (\phi\nabla^2 G - G\nabla^2\phi)dv = \int_\Gamma \left(\phi\frac{\partial G}{\partial n} - G\frac{\partial\phi}{\partial n}\right)d\Gamma. \tag{12}$$

Moving the source point s toward the boundary, we have the boundary integral equation

$$c(S)\phi(S) + \int_\Gamma \phi(S)\frac{\partial G(S, Q)}{\partial n}d\Gamma = \int_\Gamma G(S, Q)\frac{\partial\phi(S)}{\partial n}d\Gamma, \tag{13}$$

where c is a coefficient from the geometry defined as

$$c(S) = -\int_\Gamma \frac{\partial G(S, Q)}{\partial n}d\Gamma. \tag{14}$$

In this study, the isoparametric quadrilateral linear element showed in Fig. 3 is utilized. For discretization, the geometrical or physical function f on the boundary can be expressed as

$$f(\zeta_1, \zeta_2) = \sum_{k=1}^{4} \varphi_k(\zeta_1, \zeta_2) f_k, \tag{15}$$

where ζ_1, and ζ_2 are the local element coordinates, $\varphi_k(\zeta_1, \zeta_2)$ is the linear quadrilateral element shape function and f_k is the relative function value on the node in each element. Then the derivative of

function f on the boundary element is defined as

$$\frac{\partial f(\zeta_1, \zeta_2)}{\partial \zeta_i} = \sum_{k=1}^{4} \frac{\partial \varphi_k(\zeta_1, \zeta_2)}{\partial \zeta_i} f_k, \quad i=1,2. \tag{16}$$

After the boundaries being discretized, Eq. (13) can be treated by the boundary element method.

IV. LAGRANGIAN DESCRIPTION AND BASE SHEAR FORCE

In this section, the Lagrangian description is applied at the free surface only. When the liquid tank is subjected to a forced ground motion, the free surface position and the velocity potential change with time. We use the Taylor series expansion with Lagrangian description to catch the new position of the free surface and to calculate its relevant boundary properties, when the time marches. Between the time step t and $t+\Delta t$, in which Δt is a small time increment, a particle (ξ, ς, η) on the free surface at time t will move to its new position (ξ', ς', η') at time $t+\Delta t$ as shown in Fig. 4. We trace this particle and its velocity potential by the Taylor series expansion

$$\xi_i' = \xi_i + \Delta t \frac{D\xi_i}{Dt} + \frac{\Delta t^2}{2} \frac{D^2\xi_i}{Dt^2} + O[(\Delta t)^3], \; i=1, 2, 3, \tag{17}$$

$$\phi' = \phi + \Delta t \frac{D\phi}{Dt} + \frac{\Delta t^2}{2} \frac{D^2\phi}{Dt^2} + O[(\Delta t)^3], \tag{18}$$

where $\xi_1=\xi$, $\xi_2=\varsigma$ and $\xi_3=\eta$.

At each time step, we first solve the velocity potential or its normal derivative from the boundary integral equation described in the previous section. Then, we apply the Lagrangian description in succession to predict the new position of the free surface by Eqs. (17) and (18) to update the velocity potential at the next time step. In this study, the second-order expansion is adopted, and the higher order terms are dropped.

For calculating the time derivative terms in the previous Taylor series expansion equations, we must know the normal and tangential vectors at each node on the free surface elements. Therefore, a few intermediate steps are needed and described in the following. First, we have to establish a local orthogonal coordinate of each free surface node. Referring to Fig. 3, $\vec{s}_1$ is a unit tangential vector to the local element coordinate ζ_1 at one node, and $\vec{n}$ is the outward unit normal vector at the same node. Because $\vec{s}_1$ and $\vec{n}$ are perpendicular, the orthogonal vector $\vec{s}_2$ can be obtained by the cross product of $\vec{s}_1$ and $\vec{n}$. These three vectors are perpendicular to each other, then we define s_1, s_2 and n to be the corresponding local orthogonal coordinates. By these

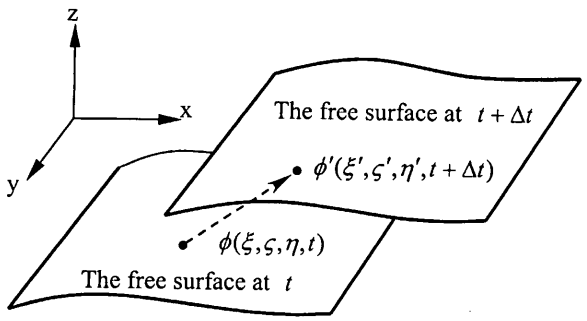

Fig. 4 The particle movement on the free surface from t to $t+\Delta t$

definitions, the tangential derivatives of a function f can be written as:

$$\frac{\partial f}{\partial s_1} = \frac{\partial \zeta_1}{\partial s_1}\frac{\partial}{\partial \zeta_1} f + \frac{\partial \zeta_2}{\partial s_1}\frac{\partial}{\partial \zeta_2} f, \tag{19}$$

$$\frac{\partial f}{\partial s_2} = \frac{\partial \zeta_1}{\partial s_2}\frac{\partial}{\partial \zeta_1} f + \frac{\partial \zeta_2}{\partial s_2}\frac{\partial}{\partial \zeta_2} f, \tag{20}$$

Hence the derivative terms between global and local coordinates are related as

$$\frac{\partial}{\partial x_i} = N_i \frac{\partial}{\partial n} + S_{1i}\frac{\partial}{\partial s_1} + S_{2i}\frac{\partial}{\partial s_2}, \tag{21}$$

in which N_i, S_{1i}, and S_{2i} are the components of unit normal and unit tangential vectors in x, y, and z directions, respectively. From Eqs. (6) and (8), we have the first-order Lagrangian time derivative of the position (i.e. velocity components) at every surface node in global coordinates:

$$\frac{D\xi_i}{Dt} = U_i = \frac{\partial \phi}{\partial x_i} = N_i \frac{\partial \phi}{\partial n} + S_{1i}\frac{\partial \phi}{\partial s_1} + S_{2i}\frac{\partial \phi}{\partial s_2}, \tag{22}$$

and

$$\frac{D\phi}{Dt} = -g\eta + \frac{1}{2} U_i U_i, \tag{23}$$

in which U_i are the velocity components of a free surface particle. Next, the second order time derivatives of positions and ϕ on the free surface can be written as

$$\frac{D^2\xi_i}{Dt^2} = \frac{D}{Dt}\frac{\partial \phi}{\partial x_i} = \frac{\partial^2 \phi}{\partial t \partial x_i} + U_j \frac{\partial \phi_{,j}}{\partial x_i}, \tag{24}$$

$$\frac{D^2\phi}{Dt^2} = U_i \frac{DU_i}{Dt} - g\frac{D\eta}{Dt}. \tag{25}$$

Since ϕ is continuous everywhere in the tank, the term $\frac{\partial^2 \phi}{\partial t \partial x_i}$ in Eq. (24) can be expressed as $\frac{\partial \phi_t}{\partial x_i}$ and

$$\frac{\partial \phi_t}{\partial x_i} = N_i \frac{\partial \phi_t}{\partial n} + S_{1i} \frac{\partial \phi_t}{\partial s_1} + S_{2i} \frac{\partial \phi_t}{\partial s_2}, \tag{26}$$

where ϕ_t on the free surface is calculated from Eq. (7). Because ϕ_t in the computational domain satisfies the Laplace equation, we can use the same idea mentioned in the previous section to solve the boundary value problems such as

$$\nabla^2 \phi_t = 0$$

$$\phi_t = \textit{specified, on free surface,} \tag{27}$$

$$\frac{\partial \phi_t}{\partial n} = \textit{specified, on lateral wall and bottom}$$

Then the unknown value $\partial \phi_t / \partial n$ on the free surface will be solved. In this kind of problem, it is not necessary to do any more integration for solving $\partial \phi_t / \partial n$, because the coefficient matrix for Eq. (13) is exactly the same as that for Eq. (27) in the same time step. Even for higher time derivatives, such as $\nabla^2 \phi_{tt} = 0$, $\nabla^2 \phi_{ttt} = 0$... etc., the coefficient matrix is still the same as for the Laplace equation. Therefore, by BEM, the computational procedure is very time economical. The other terms $\frac{\partial \phi_{,j}}{\partial x_i}$ in Eq. (24) can be represented as

$$\frac{\partial \phi_{,j}}{\partial x_i} = N_i \frac{\partial \phi_{,j}}{\partial n} + S_{1i} \frac{\partial \phi_{,j}}{\partial s_1} + S_{2i} \frac{\partial \phi_{,j}}{\partial s_2}. \tag{28}$$

Further expanding the above equation, we have

$$\frac{\partial \phi_{,j}}{\partial n} = \frac{\partial \phi_{,n}}{\partial x_j} = N_j \frac{\partial}{\partial n}\frac{\partial \phi}{\partial n} + S_{1j} \frac{\partial}{\partial s_1}\frac{\partial \phi}{\partial n} + S_{2j} \frac{\partial}{\partial s_2}\frac{\partial \phi}{\partial n} \tag{29}$$

$$\frac{\partial \phi_{,j}}{\partial s_1} = \frac{\partial \phi_{,s_1}}{\partial x_j} = N_j \frac{\partial}{\partial n}\frac{\partial \phi}{\partial s_1} + S_{1j} \frac{\partial}{\partial s_1}\frac{\partial \phi}{\partial s_1} + S_{2j} \frac{\partial}{\partial s_2}\frac{\partial \phi}{\partial s_1} \tag{30}$$

$$\frac{\partial \phi_{,j}}{\partial s_2} = \frac{\partial \phi_{,s_2}}{\partial x_j} = N_j \frac{\partial}{\partial n}\frac{\partial \phi}{\partial s_2} + S_{1j} \frac{\partial}{\partial s_1}\frac{\partial \phi}{\partial s_2} + S_{2j} \frac{\partial}{\partial s_2}\frac{\partial \phi}{\partial s_2} \tag{31}$$

With previous calculation, all the terms except $\frac{\partial^2 \phi}{\partial n^2}$ in Eqs. (29)~(31) can be evaluated one by one on local elements. Finally, the term $\frac{\partial^2 \phi}{\partial n^2}$ is computed through the Laplace equation such that

$$\frac{\partial^2 \phi}{\partial n^2} = -\left(\frac{\partial^2 \phi}{\partial s_1^2} + \frac{\partial^2 \phi}{\partial s_2^2}\right). \tag{32}$$

Up to now, all the terms in the second-order TSE method can be carried out successfully.

After the calculation of the free surface movement, the hydrodynamic pressure on the lateral wall can be evaluated from Bernoulli's Equation

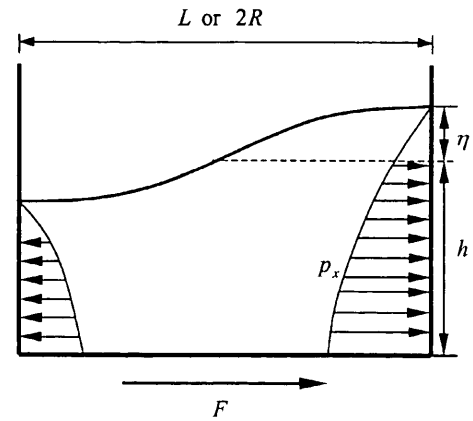

Fig. 5 Base shear force due to the hydrodynamic pressure

$$p(x, y, z, t) = -\rho\left(\frac{\partial \phi}{\partial t} + \frac{1}{2}(\nabla \phi)^2 + gz\right). \tag{33}$$

Then, the base shear force F due to the difference of hydrodynamic pressures in the x-direction on the vertical wall shown in Fig. 5 can be calculated by

$$F = \int_{\Gamma_w} p_x d\Gamma_w. \tag{34}$$

In Eq. (34), p_x is the x-directional hydrodynamic pressure on the vertical side wall.

V. NUMERICAL EXAMPLES

The first example in this study is a three-dimensional rectangular tank, partially-filled with water, subjected to x-direction forced motion. Fig. 1 shows a three-dimensional rectangular tank. In order to check the accuracy of the numerical result the analytical solution of the hydrodynamic pressure from an accelerating rectangular tank, developed by Chwang and Wang (1984), is adopted for comparison. The nondimensional pressure is defined as

$$C_p = \frac{p(x, y, z, t)}{\rho a h}, \tag{35}$$

where a represents the constant acceleration applied to the tank. While $t=0$, the distribution of C_p on $x=0$ is expressed as

$$C_p = 2 \sum_{m=1}^{\infty} \frac{(-1)^m (1 - \cosh k_m L)}{k_m^2 h^2 \sinh k_m L} \cos k_m z, \tag{36}$$

in which

$$k_m = \frac{(2m-1)\pi}{2h} \quad (m = 1, 2, 3, \ldots).$$

Figure 6 shows the results of present work and the analytical solution of C_p for $L/h = 1.0$ and $a = 0.2g$. The

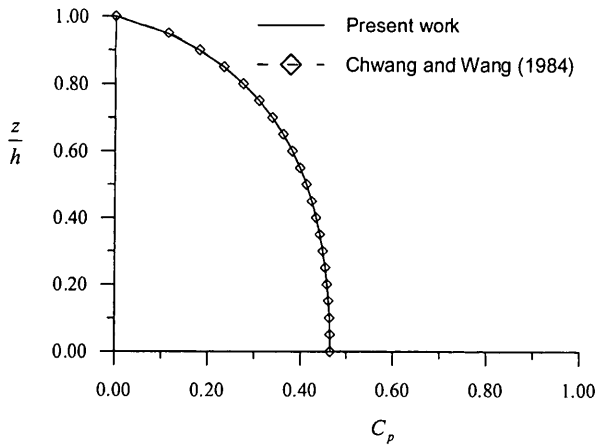

Fig. 6 The hydrodynamic pressure distribution on the left side wall

agreement between these two results is very good.

Then, a three-dimensional rectangular tank subjected to horizontal harmonic forced oscillation will be calculated. The length of the tank is 0.9m, the width is 0.3m and the still water depth is 0.6m. By the linear wave theorem (Currie, 1993), the first natural frequency is

$$\omega_1 = \sqrt{\frac{\pi g}{L}\tanh\frac{\pi h}{L}} \,. \tag{37}$$

Thus the first natural frequency of this tank is

$$\omega_1 = 5.761 \text{ rad/sec.}$$

Because this tank is subjected to a harmonic forced oscillation, the lateral boundary conditions of the right side Γ_r and left side Γ_l of the tank are

$$\frac{\partial \phi}{\partial n} = V = \pm \omega_f x_0 \sin \omega_f t, \quad \text{on } \Gamma_r \text{ and } \Gamma_l, \tag{38}$$

in which ω_f is the forced frequency and x_0 is the amplitude of the tank oscillation. The boundary condition of the bottom is

$$\frac{\partial \phi}{\partial n} = 0$$

In this study, the free surface wave and base shear force at different forced frequency are most concerned. There are two different forced frequencies denoted as 5.0 rad/sec and 5.5 rad/sec. In the computation, the forced displacement amplitude is 0.003636 m, the time increment is 0.001 sec, and the boundary is meshed into 600 quadrilateral linear elements (18, 6, and 8 meshes along x, y, and z directions, respectively).

The time history of the elevation of the free surface at the right side wall of the tank is plotted in Fig. 7. The result of the case, ω_f=5.5 rad/sec, is very consistent with that of the two-dimensional computation by Liu *et al.* (1992). In this case, the wave amplitude at the wall increases almost linearly. This forced frequency is very close to the first natural frequency of the water tank, thus the resonance phenomenon is very significant. By the potential flow assumptions, the wave height grows linearly and seems like a divergence condition at resonance in our calculation, but an artificial experimental Rayleigth damping term can be added into the dynamic boundary condition (i.e. Eq. (7)) for practical engineering applications (Nakayama and Washizu, 1981). The other forced frequency, ω_f=5.0 rad/sec, is far away from the resonance frequency, so the amplitude of the free surface wave is more calming and a "surf beat" phenomenon appears (Liu *et al.*, 1992). Fig. 8 shows the time history of base shear forces due to the hydrodynamic pressure. In the above examples, when the excited frequency is far enough from the resonant frequency, the amplitude of waves doesn't grow. Basically, it means the present numerical method is stable. However, when the excited frequency is near the resonant frequency, the growth of wave height is

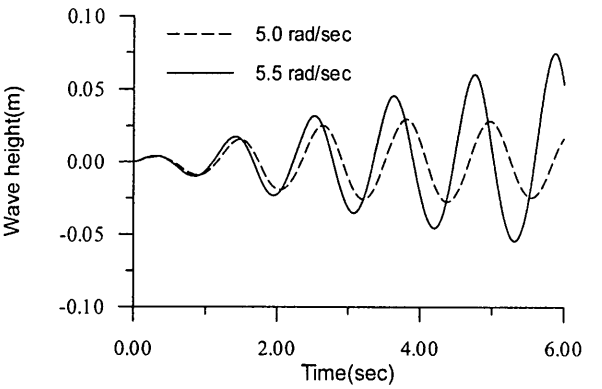

Fig. 7 Free surface height at the right lateral wall of the rectangular tank

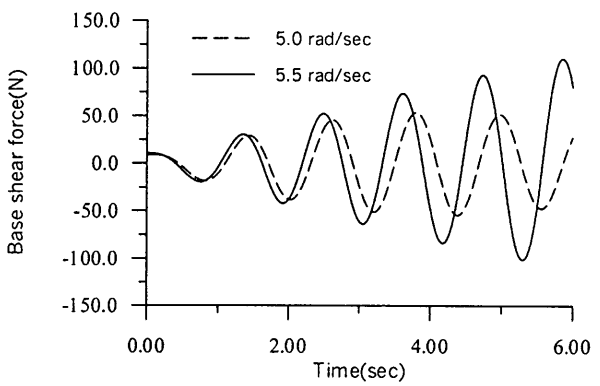

Fig. 8 The base shear force of the rectangular tank

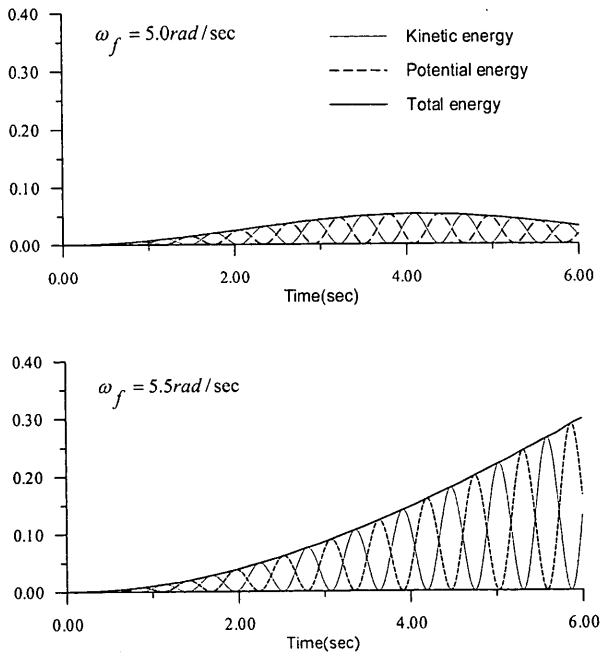

Fig. 9 Normalized energy for the rectangular tank

the nature of physical phenomena. The larger base shear force also occurs when the frequency is close to the resonance ω_f=5.5 rad/sec. This means that the tank will provide significant base shear force at resonance. The normalized energy for each forced frequency is plotted in Fig. 9. The normalized kinetic energy is

$$E_k = \frac{1}{2gA_f x_0}\int_{\Gamma_f} \phi \frac{\partial \phi}{\partial n} d\Gamma_f, \tag{39}$$

where A_f is the free surface area at rest, and the normalized potential energy is

$$E_p = \frac{1}{2A_f x_0}\int_{\Gamma_f} \eta^2 d\Gamma_f. \tag{40}$$

The total energy at ω_f=5.5 rad/sec is much larger than that at ω_f=5.0 rad/sec. This result also shows that a TLD will have good vibration reduction at the resonance condition. Fig. 10 is a typical sloshing mode calculated by the present method. There is almost no change along the y-direction, because it is actually a two-dimensional problem.

Figure 11 shows a cylindrical water tank. The horizontal harmonic forced vibration is also concerned here. The still water depth is 0.48 m, and the radius is 0.33 m. By the linear wave theorem (Currie, 1993), the natural frequency of a cylindrical water tank is

$$\omega_j = \sqrt{\frac{\lambda_j g}{R}\tanh\left(\lambda_j \frac{h}{R}\right)}. \tag{41}$$

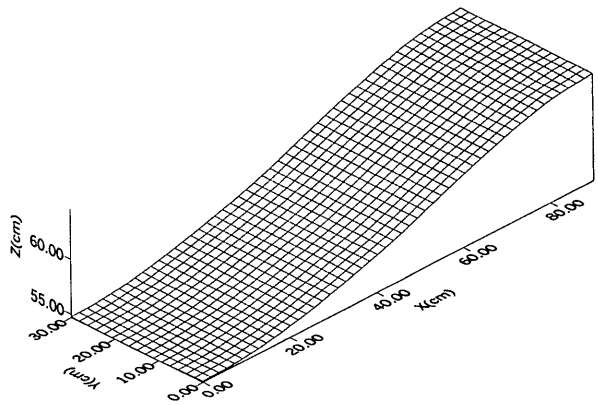

Fig. 10 The calculated sloshing shape of the free surface wave in the rectangular tank

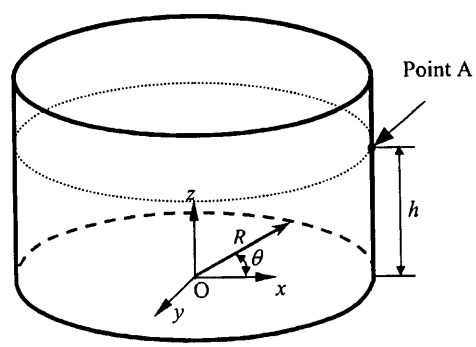

Fig. 11 The cylindrical tank

λ_j is the values when the first derivative of the first order Bessell function ($J_1'(\lambda_j)$) is zero. Considering the first-mode wave motion in this tank, λ_1=1.841 is selected and the lowest natural frequency of wave motion is 5.66rad/sec. From the given forced vibration, the lateral boundary condition on the side wall of the tank is

$$\frac{\partial \phi}{\partial n} = V = \omega_f x_0 \sin\omega_f t \cos(\theta), \quad \text{on } \Gamma_w, \tag{42}$$

and the boundary condition of bottom is

$$\frac{\partial \phi}{\partial n} = 0.$$

Two forced frequencies 5.0 rad/sec and 5.5 rad/sec are also chosen, the forced displacement amplitude is 0.003636 m, the time increment is 0.001 sec, and the boundary is meshed into 320 quadrilateral linear elements (112 elements on the free surface or bottom, 96 elements on the lateral wall, respectively).

Figure 12 shows the time history of the free surface wave elevation at point A which is indicated in Fig. 11. The wave amplitude grows almost linearly for ω_f=5.5 rad/sec and the "surf beat" phenomenon also appears at ω_f=5.0 rad/sec. Fig. 13 and Fig. 14 are the plots of time histories of the base shear force

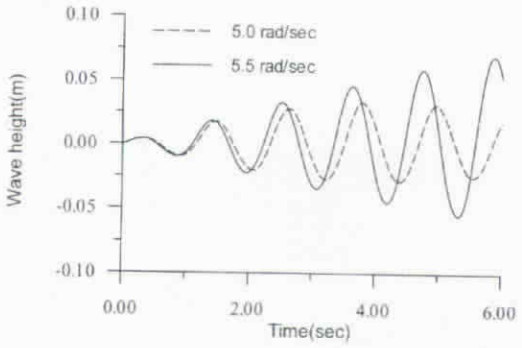

Fig. 12 Free surface at point A of the cylindrical tank

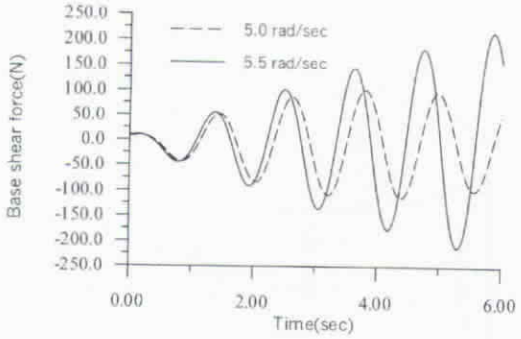

Fig. 13 The base shear force of the cylindrical tank

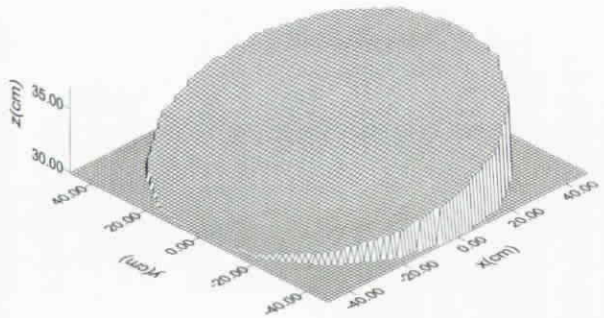

Fig. 15 The sloshing shape of the free surface wave in the cylindrical tank at t=3.5 sec and ω_f=5.5 rad/sec

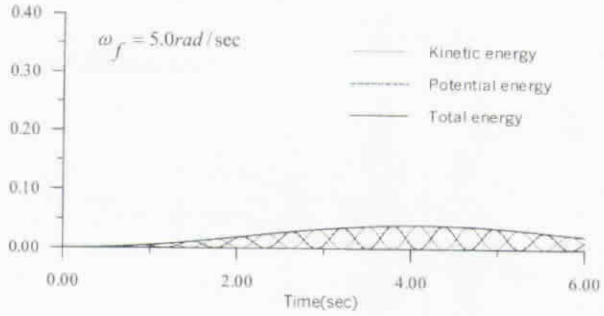

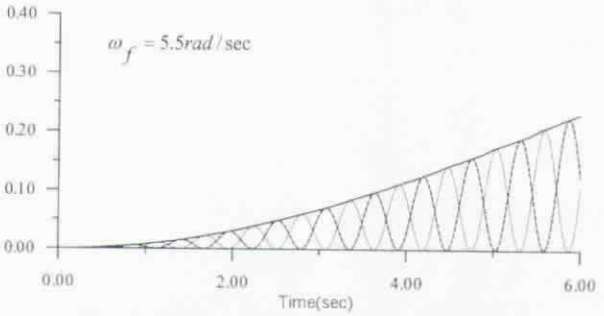

Fig. 14 Normalized energy for the cylindrical tank

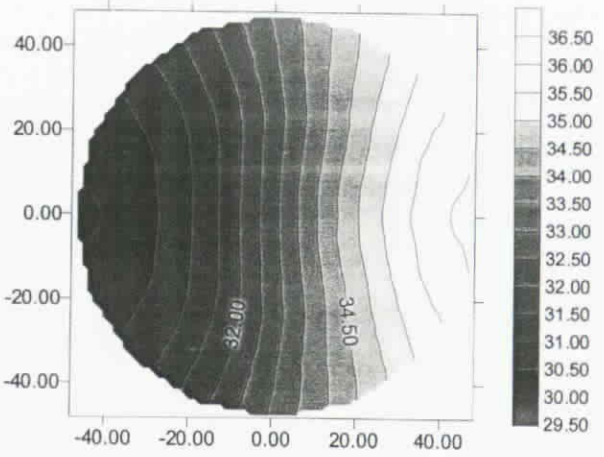

Fig. 16 The contour of the free surface wave in the cylindrical tank (unit:cm)

and the normalized energy. The tank also provides lager base shear forces and more total energy at resonance. Fig. 15 shows the calculated free-surface sloshing shape in a cylindrical tank at t=3.5 sec and ω_f=5.5 rad/sec. Fig. 16 shows the wave contour lines, from which we can find that the free surface wave distribution is three-dimensional and symmetrical about the central x-z plane. The non-linear behavior has also been shown by the contour lines in the figure. Fig. 17 shows the free surface profile along the central x-z plane in the cylindrical tank at time t=0 sec, t=1.5 sec, and t=3.5 sec respectively.

From Eq. (33), the lateral hydrodynamic pressure is the sum of the following terms: $-\rho\dfrac{\partial\phi}{\partial t}$, $-\dfrac{\rho}{2}(\nabla\phi)^2$ and $-\rho gz$. Thus the base shear force F can also be considered as the sum of the three components and assigned as F_1, F_2 and F_3. The result of the three components in a cylindrical tank is plotted in Fig. 18. It is very interesting that the base shear force is most dominated by the first term, namely inertial force, and, the other terms can be neglected. The base shear force per unit weight of water (N/kg) at ω_f= 5.5rad/sec of the rectangular and cylindrical tanks are compared and shown in Fig. 19. It shows that the cylindrical tank could also provide significant base shear force, which means that the cylindrical tank would also have excellent performance in vibration

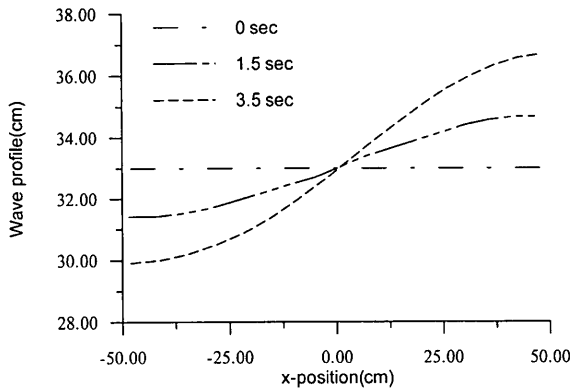

Fig. 17 The free surface wave profile along the central x-z plane in the cylindrical tank at ω_f=5.5 sec/rad

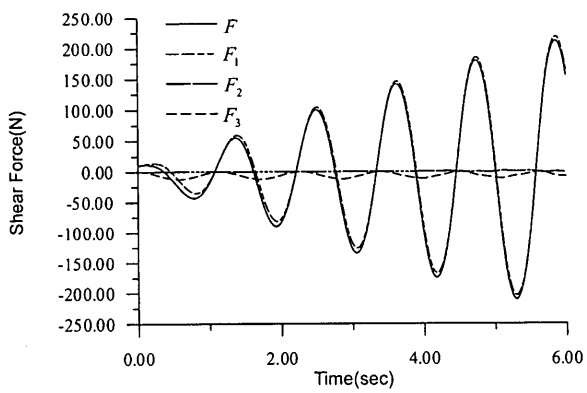

Fig. 18 The three components of the base shear force of a cylindrical tank at ω_f=5.5 rad/sec (F: total force, F_1: due to $-\rho\partial\phi/\partial t$, F_2: due to $-\rho(\nabla\phi)^2/2$, and F_3: due to $-\rho gz$)

reduction. More examples' calculations and experiences will be required for further comparisons of the rectangular and cylindrical TLD's.

VI. CONCLUSION

The numerical method using BEM with TSE and Lagrangian description for the calculation of the transient solution (or the time history) of the three-dimensional nonlinear water sloshing problem of a TLD is developed. The comparison of the results between a three-dimensional rectangular TLD calculated by the present work and a two-dimensional one calculated by Chwang and Wang (1984), and by Liu *et al.* (1992) show good agreement. The behavior of water sloshing in a cylindrical tank has also been predicted successfully. Therefore it can be said that this algorithm is reliable and practical for dealing with the three- dimensional nonlinear sloshing problems of TLD's.

From the examples' results given in this paper, a TLD has significant base shear forces at resonance,

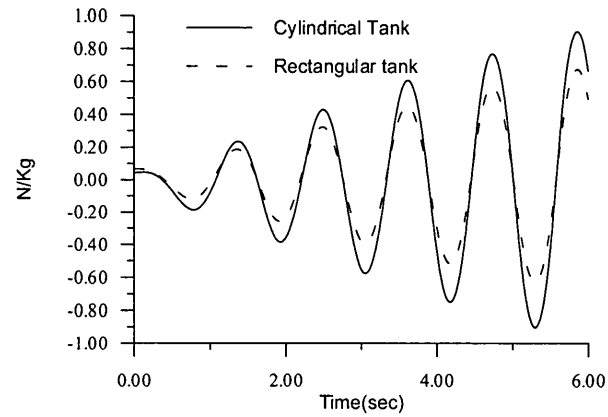

Fig. 19 The unit base shear force per unit weight of water at ω_f= 5.5 rad/sec of the cylindrical tank and rectangular tank

and the inertia force dominates the base shear force mostly. The results also show that both the rectangular and cylindrical TLD's could have excellent vibration reduction with regard to their main structures. The present method can successfully predict both wave height and base shear forces at resonance conditions for any three-dimensional TLD's to the harmonic forced oscillation. It could also be applied to the three-dimensional nonlinear sloshing problem of a TLD subject to other kinds of horizontal forced oscillation, such as horizontal earthquake records. More calculations, model tests, and engineering applications should be examined for future study.

ACKNOWLEDGEMENT

The authors gratefully acknowledge the sponsorship of this research project by the National Science Council of the Republic of China under the Grant NSC-87-2211-E-002-072.

REFERENCE

1. Abe, K., and Kamio, T., 1994, "Two-Dimensional Nonlinear Sloshing Analysis Using Boundary Element Method," *Proceeding of JSCE*, No. 489/I -27, pp. 111-120 (In Japanese).
2. Aslam, M., 1981, "Finite Element Analysis of Earthquake-Induced Sloshing in Axisymmetric Tanks," *International Journal for Numerical Methods in Engineering*, Vol. 17, pp. 159-170.
3. Broeze, J., Van Daalen E.F.G., and Zandbergen, P.J., 1993, "A Three-Dimensional Panel Method for Nonlinear Free Surface Waves on Vector Computer," *Computational Mechanics*, Vol. 13, pp. 12-28.
4. Bühmann, B., Skrourup J., and Cheung, K.F., 1998, "Run-up on a Structure due to second-order waves and a current in a numerical wave

tank," *Applied Ocean Research*, Vol. 20, pp. 297-308.
5. Chen, Y.H., and Hwang, W.S., 1994, "Study of the Interaction in Anti-Vibrational Liquid Tank and High-Rise Building", NSC-83-0410-E002-052, Report of the National Science Council, R. O.C. (In Chinese).
6. Chen, Y.H., Hwang, W.S., Chiu, L.T., and Sheu, S. M., 1995, "Flexibility of TLD to Building by Simple Experiment and Comparison," *Computers and Structures*, Vol. 57, No. 5, pp. 855-861.
7. Chwang, Allen T., and Wang, K.H., 1984, "Nonlinear Impulsive Force on an Accelerating Container," *Journal of Fluids Engineering*, Vol. 106, pp. 233-239.
8. Currie, I.G., 1993, Fundamental Mechanics of Fluids, McGraw-Hill Inc.
9. Faltinsen O., 1974, "A Nonlinear Theory of Sloshing in Rectangular Tanks," *Journal of Ship Research*, Vol. 18, No. 4, pp. 224-241.
10. Grilli, S.T., and Subramanya, R., 1996, "Numerical Modeling of Wave Breaking by Fixed or Moving Boundaries," *Computational Mechanics*, Vol. 17, pp. 374-391.
11. Grilli, S.T., Skourup, J., and Svendsen, I.A., 1989, "An Efficient Boundary Element Method for Nonlinear Water Waves," *Engineering Analysis with Boundary Elements*, Vol. 6, No. 2, pp. 97-107.
12. Ikeda T., and Nakagawa N., 1997, "Non-Linear Vibration of a Structure Caused by Water Sloshing in a Rectangular Tank," *Journal of Sound and Vibration*, Vol. 201, No. 1, pp. 23-41.
13. Liu, Philip L.-F., Hsu, H.-W., and Lean Meng H., 1992, "Applications of Boundary Integral Equation Methods for Two-Dimensional Non-Linear Water Wave Problems," *International Journal for Numerical Methods in Fluids*, Vol. 15, pp. 1119-1141.
14. Liu, Z., and Huang, Y., 1994, "A New Method for Large Amplitude Sloshing Problems," *Journal of Sound and Vibration*, Vol. 175, No. 2, pp. 185-195.
15. Machane, R., and Canot, E., 1997, "High-Order Schemes in Boundary Element Methods for Transient Non-Linear Free Surface Problems," *International Journal for Numerical Methods in Fluids*, Vol. 24, pp. 1049-1072.
16. Nakayama, T., 1990, "A Computational Method for Simulating Transient Motions of An Incompressible Inviscid Fluid with A Free Surface," *International Journal for Numerical Methods in Fluids*, Vol. 10, pp. 683-695.
17. Nakayama, T. and Washizu, K., 1981, "The Boundary Element Method Applied to the Analysis of Two-Dimensional Nonlinear Sloshing Problems," *International Journal for Numerical Methods in Engineering*, Vol. 17, pp. 1631-1646.
18. Velestos, A.S., 1984, "Seismic Response and Design of Liquid Storage Tanks," Guidelines for the Seismic Design of Oil and Gas Pipeline Systems, ASCE.

Discussions of this paper may appear in the discussion section of a future issue. All discussions should be submitted to the Editor-in-Chief.

Manuscript Received: Dec. 01, 1999
Revision Received: Jan. 29, 2000
and Accepted: Feb. 20, 2000

應用邊界元素法於三維水沖激問題之數值模擬

陳永祥[1,2] 黃維信[2] 葛家豪[1]

[1]國立台灣大學土木工程學研究所
[2]國立台灣大學造船及海洋工程學研究所

摘 要

本研究主要探討三維諧調液體阻尼器（Tuned Liquid Damper，或簡稱TLD）之水槽承受水平強制振動時，內部液體之非線性沖激（sloshing）行爲。本研究應用三維邊界元素法，配合二階泰勒級數展開（Taylor series expansion）和Langrangian座標描述以計算並追踪當TLD受強制振動時其自由液面變化及液體質點運動。本研究以三維矩形及圓柱型水槽爲算例，探討其受簡諧水平振動時，內部液體之沖激歷時反應及所產生的底部剪力。

關鍵詞：邊界元素法，液體沖激，諧調液體阻尼器。